

# Cubic Spline Interpolation with Overlapped Window and Data Reuse for On-line Hilbert Huang Transform Biomedical Microprocessor

Nai-Fu Chang, Cheng-Yi Chiang, Tung-Chien Chen and Liang-Gee Chen

**Abstract**— On-chip implementation of Hilbert-Huang transform (HHT) has great impact to analyze the non-linear and non-stationary biomedical signals on wearable or implantable sensors for the real-time applications. Cubic spline interpolation (CSI) consumes the most computation in HHT, and is the key component for the HHT processor. In tradition, CSI in HHT is usually performed after the collection of a large window of signals, and the long latency violates the realtime requirement of the applications. In this work, we propose to keep processing the incoming signals on-line with small and overlapped data windows without sacrificing the interpolation accuracy. 58% multiplication and 73% division of CSI are saved after the data reuse between the data windows.

## I. INTRODUCTION

Most of biomedical signals, e.g. electroencephalogram (EEG) and electrocardiogram (ECG), exhibit significant complex behavior with strong non-linear and non-stationary properties [1][2]. Fourier Transform works on a priori basis of assumption that the processed signals are linear and stationary [3]. The difficulty of the wavelet analysis is its non-adaptive nature [3]. Hilbert-Huang Transform (HHT), proposed by Huang et al. [3], is an adaptive data analysis method and provides a possible solution for non-linear and non-stationary signal analysis. Recently, HHT has been widely used for biomedical engineering, such as sleep analysis [4], brain computer interface (BCI) [5], noise removing [6] and seizure prediction [7].

The VLSI on-chip system is the current trend because of the power and area constraints imposed by the wearable or implantable devices. As front-end and wireless circuits are acquirable, signal processors are needed to complete the real-time applications. On-chip systems for some of the key signal processing algorithms, such as finite impulse response (FIR) filter, fast Fourier transform (FFT), discrete wavelet transform (DWT), and so on., have been proposed [8][9][10]. HHT is a crucial work but its on-chip system has not been implemented so far.

HHT is the combination of the empirical mode decomposition (EMD) and the Hilbert spectral analysis. The key part of the algorithm is the EMD method, in which cubic spline interpolation (CSI) consumes the most computation. Due to the computation need of the heavy sifting process in the EMD, the algorithm is often used off-line through personal computer (PC). The sequential flow and the high computation

to solve the tridiagonal matrix algorithm (TDMA) for CSI makes on-line EMD difficult. Therefore, an on-line interpolation method with low computation is required for EMD microprocessor.

In this paper, a cubic spline interpolation method with overlapped window and data reuse is proposed to support on-line HHT biomedical microprocessor with only negligible penalty in accuracy. The remainder of this paper is organized as follows. Section II briefly reviews the theory of the EMD algorithm and the CSI algorithm which will be used in the computation of the EMD algorithm. The design issues and the proposed interpolation method are described in Section III. The implementation results are shown in Section IV. Finally, Section V describes the conclusion and the future works.

## II. ALGORITHM

The EMD method, proposed by Huang et al. [3], is the fundamental part of the HHT. It uses the cubic spline interpolation (CSI) algorithm. Before the interpolation method for the on-line HHT, we will briefly review the EMD method and the CSI algorithm in this section.

### A. Empirical Mode Decomposition

The EMD method decomposes the complicated data set into a finite and often small number of components. These components are intrinsic mode functions (IMFs). An IMF represents a generally simple oscillatory mode as a counterpart to the simple harmonic function. By definition, an IMF satisfies two conditions.

- a) The number of extrema and the number of zero-crossings must be either equal or differ at most by one in the whole data set.
- b) At any point, the mean value of the envelope defined by the local maxima and the envelope defined by local minima is zero.

Given a signal  $x(t)$ , the sifting process of EMD can be summarized in the following steps.

- 1) Identify the local maxima and minima of  $x(t)$ .
- 2) Generate the upper envelope  $U(t)$  and the lower envelope  $L(t)$  via CSI among all the maxima and minima, respectively.
- 3) Compute the average of the two envelopes. The average is defined as  $m(t) = (U(t) + L(t))/2$ .
- 4) Subtract  $m(t)$  from the data to obtain an IMF candidate, that is  $c(t) = x(t) - m(t)$ .
- 5) Check if  $c(t)$  satisfies the defined properties of IMF. If properties are satisfied,  $c(t)$  can be regarded as an IMF.

We thank Fang-Chia Chang for providing rat EEG data, and School of Veterinary Medicine National Taiwan University.

N.-F. Chang, C.-Y. Chiang, T.-C. Chen and L.-G. Chen are with the DSP/IC Design Lab, Graduate Institute of Electronics Engineering, National Taiwan University, Taipei, Taiwan. (e-mail: knife@video.ee.ntu.edu.tw).

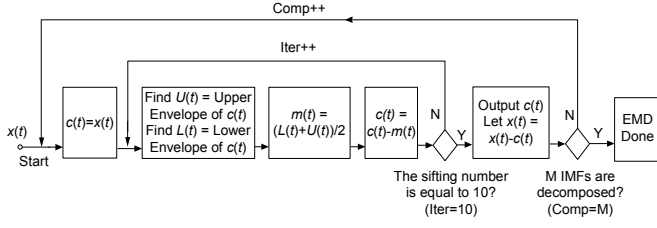


Fig. 1. The flow chart shows the EMD sifting process. There are two main loops-the component loop and the iteration loop as well as two parameters, e.g. the window length  $W$  of the signal and the number of IMFs  $M$  in the EMD algorithm.

If not, the step 1-4 should be repeated until the terminate properties are fulfilled.

6) Evaluate the residue  $r(t)$  by separating the IMF  $c(t)$  from original signal  $x(t)$  as  $r(t) = x(t) - c(t)$ .

7) Take  $r(t)$  as input data and repeat step 1-6, and obtain a number of IMFs until the properties of (a) and (b) are fulfilled.

After EMD sifting process, the signals can be represented as the sums of several IMFs from the high-frequency part to the low-frequency part and the residue.

$$x(t) = r(t) + \sum_{i=1}^n c_i(t), \quad (1)$$

where  $n$  is the number of IMF components.

There are several termination criteria of IMFs. These criteria lead to a common undesired feature that the decomposition is sensitive to the local perturbation and to the addition of new data. To solve the problem, Wu and Huang [11] proposed to fix the sifting number for the decomposition. The sifting number is 10 to guarantee the stability and convergence of the resulting IMFs.

Fig. 1 shows the flow of EMD sifting process. There are two main loops in each EMD sifting process - the component loop and the iteration loop. There are two parameters in the EMD algorithm, such as the window length  $W$  of the signal and the number of IMFs  $M$ . In practice, these parameters are set according to different applications and demands. For example, the number of IMFs, usually used to analyze EEG/ECG signals, is about two to five.

### B. Cubic Spline Interpolation

CSI is applied to connect the maxima and the minima in the EMD process. Suppose a set of  $n$  maxima (minima) is denoted by  $m_1, m_2, \dots$  and  $m_n$  with sample numbers  $t_1, t_2, \dots$  and  $t_n$ , piecewise third degree polynomial functions are used to present the  $n - 1$  intervals between  $n$  maxima (minima). We can write the equations of these functions as follows,

$$M_i(t) = a_i t^3 + b_i t^2 + c_i t + d_i, \quad (2)$$

where  $t \in [0, t_{i+1} - t_i]$  and  $i = 1, 2, \dots, n-1$ . The third order polynomial functions, called cubic splines, must satisfy three constraints.  $m_i, M'_i$  and  $M''_i$  are continuous on the interval  $[t_1, t_n]$ .

Then, equations can be written as follow:

$$\begin{aligned} m_i &= M_i(0) = M_{i-1}(t_i - t_{i-1}) \\ M'_i(0) &= M'_{i-1}(t_i - t_{i-1}) \\ M''_i(0) &= M''_{i-1}(t_i - t_{i-1}). \end{aligned} \quad (3)$$

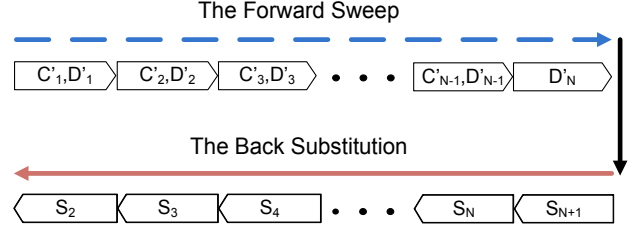


Fig. 2. The schedule of the TDMA demonstrates the data dependencies on the forward sweep and the back substitution.

Assume that  $S_i$  is the function's second derivative,  $M''_i(0)$ , and  $h_i$  is the sample number difference,  $t_{i+1} - t_i$ , a tridiagonal matrix can be derived,

$$\begin{bmatrix} B_1 & C_1 & 0 & \dots & 0 & 0 \\ A_2 & B_2 & C_2 & \dots & 0 & 0 \\ 0 & A_3 & B_3 & \dots & 0 & 0 \\ \vdots & \vdots & \vdots & \ddots & \vdots & \vdots \\ 0 & 0 & 0 & \dots & B_{N-1} & C_{N-1} \\ 0 & 0 & 0 & \dots & A_N & B_N \end{bmatrix} \begin{bmatrix} S_2 \\ S_3 \\ S_4 \\ \vdots \\ S_N \\ S_{N+1} \end{bmatrix} = \begin{bmatrix} D_1 \\ D_2 \\ D_3 \\ \vdots \\ D_{N-1} \\ D_N \end{bmatrix} \quad (4)$$

where

$$\begin{aligned} N &= n - 2 \\ A_i &= h_i & \text{for } i &= 2 \sim N \\ B_i &= 2(h_i + h_{i+1}) & \text{for } i &= 1 \sim N \\ C_i &= h_i & \text{for } i &= 1 \sim N - 1 \\ D_i &= 6 \left( \frac{m_{i+2} - m_{i+1}}{h_{i+1}} - \frac{m_{i+1} - m_i}{h_i} \right) & \text{for } i &= 1 \sim N. \end{aligned} \quad (5)$$

The values of  $S_i$  can be solved by the TDMA with two steps. The first step consists of modifying the coefficients as follows, denoting the new modified coefficients with primes

$$C'_i = \begin{cases} \frac{C_i}{B_i} & \text{for } i = 1 \\ \frac{C_i}{B_i - C'_{i-1} A_i} & \text{for } i = 2 \sim N - 1 \end{cases} \quad (6)$$

and

$$D'_i = \begin{cases} \frac{D_i}{B_i} & \text{for } i = 1 \\ \frac{D_i - D'_{i-1} A_i}{B_i - C'_{i-1} A_i} & \text{for } i = 2 \sim N \end{cases} \quad (7)$$

This is the forward sweep. The solution is then obtained by the back substitution:

$$S_i = \begin{cases} D'_{i-1} & \text{for } i = N + 1 \\ D'_{i-1} - C'_{i-1} S_{i+1} & \text{for } i = N \sim 2. \end{cases} \quad (8)$$

Fig. 2 shows the data dependencies on the forward sweep and the back substitution. First, each of the modified coefficients,  $C'_i$  and  $D'_i$ , is generated iteratively. Then,  $S_i$  can be calculated after the forward sweep finishes.  $S_i$  is computed from  $S_{N+1}$  to  $S_2$  iteratively in back substitution.

The coefficients of piecewise polynomial functions can be derived by the following equations.

$$\begin{aligned} a_i &= \frac{S_{i+1} - S_i}{6h_i} \\ b_i &= \frac{S_i}{2} \\ c_i &= \frac{m_{i+1} - m_i}{h_i} - \frac{2h_i S_i + h_i S_{i+1}}{6} \\ d_i &= m_i \end{aligned} \quad (9)$$

To solve the coefficients of the splines, two additional spline boundary conditions are required. The second derivatives of the two boundary extrema,  $S_1$  and  $S_n$  are set to zeros. Finally, the interpolated samples in an interval can be computed by substituting the corresponding  $t$  into (2). For example,  $t$  are integers which ranges from 0 to  $t_4 - t_3$  in the 3<sup>rd</sup> interval between extrema  $m_3$  and  $m_4$ .

## III. PROPOSED INTERPOLATION METHOD

### A. On-line Interpolation with Overlapped Window

In general, off-line EMD processing is executed on the signals with a large window length  $W$ . It ensures that there

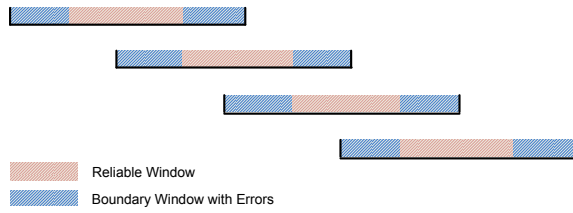


Fig. 3. The concept of on-line interpolation with overlapped windows.

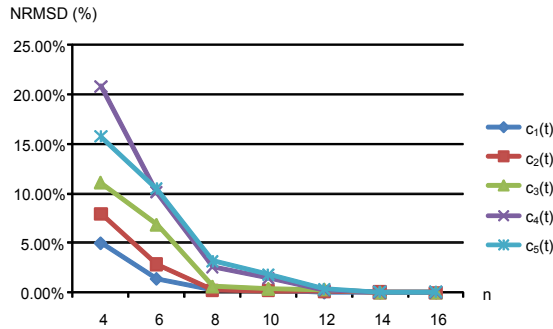


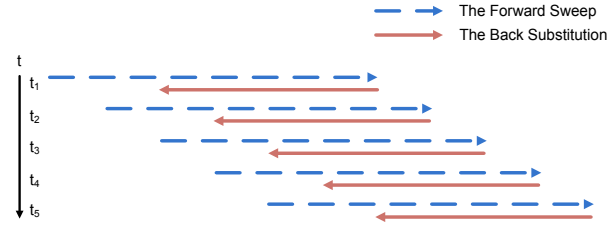
Fig. 4. The normalized root mean squared deviation (NRMSD) of IMFs interpolated on the middle interval of different  $n$  of extrema ( $n = 4, 6, 8, 10, 12, 14$  and  $16$ ).

are enough extrema to compute CSI and produce meaningful IMFs. However, data with the large window length results in high latency on data collection. On-line EMD processing is required on HHT hardware implementation. On-line EMD processing means to calculate accurate results immediately when new data is available. To have an on-line EMD, an on-line CSI method is first required.

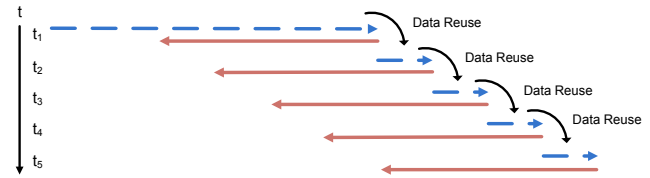
Nevertheless, the boundary intervals of the envelope might have errors because of the assumptions on boundary conditions of CSI. Due to the data dependencies of EMD, these errors would propagate between IMFs and affects accuracy of the IMF results. Thus, the results must be interpreted cautiously by determining the window within which the interpolated values are reliable. Data could be completed through overlapping the reliable windows. Fig. 3 shows the concept of on-line interpolation with overlapped windows. When new data is available, the values of reliable window are produced immediately to achieve on-line EMD. It is of great merit to lower the window size  $W$  because the latency will be decreased. While accuracy and computation loading are primary design issues to implement HHT microprocessor, the reliable window size and data reuse are applied to cope with the two issues.

### B. Determination of the Window Size

One strategy is to interpolate the intervals with smaller window length  $W$  of data, that is, to execute CSI with fewer extrema. Because the boundary intervals of the envelope might have errors, therefore, only the middle spline for  $n$  extrema CSI is adopted for interpolating the upper envelope  $U(t)$  and the lower envelope  $L(t)$ . However, larger  $n$  contributes to larger latency because more time is needed to wait for sufficient supporting extrema. To determine the optimal value of  $n$  in terms of accuracy, we use the normalized root mean squared deviation ( $NRMSD$ ) to estimate the accuracy of interpolation. We execute EMD process on a large window



(a) Interpolation Schedule Before Data Reuse



(b) Interpolation Schedule After Data Reuse

Fig. 5. The concept of data reuse applied on the revised interpolation method. The computation loading of the forward sweep reduces largely through data reuse.

as the referenced results and assume that the IMF results at the center of the large window are not affected by the end effects. These IMF results will be compared with the ones computed in the short window, centered in the large one. The large window size and short window size are 32 seconds and 4 seconds rat EEG data with the sampling rate of 256sps. The  $NRMSD$  is defined below:

$$NRMSD = \frac{RMSD}{c_{max} - c_{min}}, \quad (10)$$

where

$$RMSD = \frac{\sum_{t=0}^T |c'(t) - c(t)|^2}{T},$$

$c'(t)$  is the IMF computed by CSI on the middle interval,  $c(t)$  is the IMF using large interpolation method,  $T$  is the number of points, and  $c_{max}$  and  $c_{min}$  are the maximum and minimum values of  $c'(t)$ .

Fig. 4 shows the trend of  $NRMSD$  testing on rat EEG signals compared to CSI on the middle interval of different  $n$  extrema. The error propagates from the boundary. Therefore, as  $n$  increases, the total error is less significant and will eventually decrease to ignorable level. Due to the error propagation from previous IMFs to later IMFs and lower energy of later IMFs, later IMFs have larger errors. In our case,  $n = 8$  is chosen, while the  $NRMSD$  is below 3.5% on each IMF. The value of  $n$  changes according to different biomedical signals.

### C. Revised Interpolation Method with Data Reuse

To derive the middle spline, the original method for solving eight-extrema CSI coefficients requires large computational loading, as shown in Fig. 5(a). We decrease the computational loading by reusing the coefficients in the forward sweep. When a new extremum,  $m_M$ , is detected, only the forward sweep coefficients of last two extrema are calculated. Then, previous forward sweep coefficients are combined with the latest coefficients, as shown in Fig. 5(b). Through data reuse, the computation times of multiplication and division for the spline coefficient are reduced by 58%

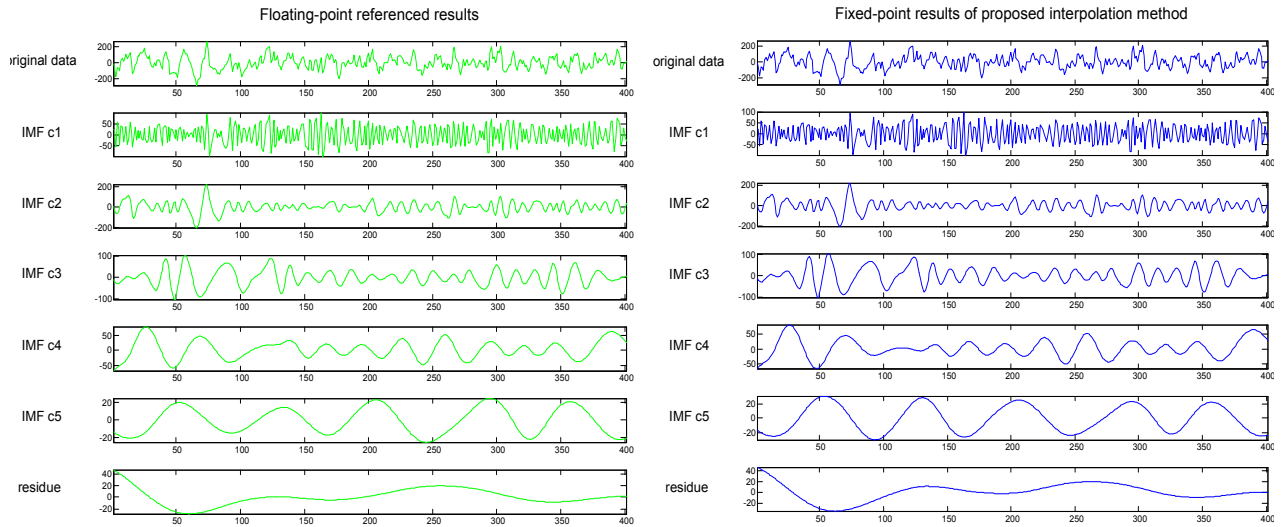


Fig. 7. The results of five IMFs and residue after empirical mode decomposition on the raw rat EEG signal. The signals with green line are the floating-point results produced by the referenced results. The signals with blue lines are the fixed-point results produced by the proposed interpolation method.

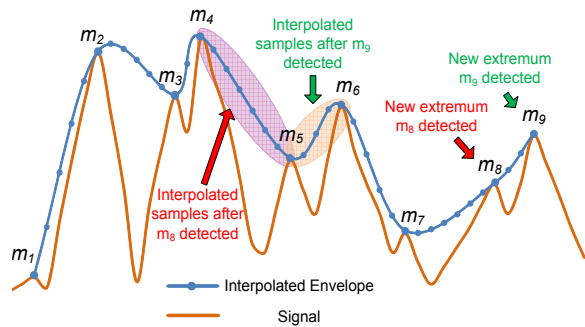


Fig. 6. Illustration on the proposed interpolation schedule.  $m_1, m_2, \dots, m_9$  are the extrema. The interval between  $m_{i-4}$  and  $m_{i-3}$  could be interpolated when a new extremum  $m_i$  is detected.

and 73% respectively. Otherwise, the effect of boundary propagation of one side is decreased as more forward data is collected.

#### D. Proposed Interpolation Schedule

Fig. 6 illustrates the interpolation schedule.  $m_1, m_2, \dots, m_9$  are the extrema. When new extremum  $m_8$  is detected, the middle interval between  $m_4$  and  $m_5$  can be generated by CSI on the the eight extrema  $m_1$  to  $m_8$ . When next extremum  $m_9$  is detected,  $m_1$  to  $m_9$  are used to interpolate the interval between  $m_5$  and  $m_6$ .

### IV. SIMULATION RESULTS

On-line EMD processing could be achieved based on the proposed on-line interpolation method. When new data become available, the corresponding upper and lower envelopes can be interpolated immediately. The IMF and its residue in the interval can be computed. The residue can then be used to do the next EMD iteration.

Fig. 7 displays the comparison. The raw rat EEG signal with the sampling rate of 256sps is decomposed into five IMFs and the residue. The green signals on the left are the floating-point referenced results, while the blue ones on the right are the fixed-point results produced by the proposed interpolation method. The *NRMSD* of each IMF result by our approach is less than 3.5%.

### V. CONCLUSION AND FUTURE WORKS

In this paper, an interpolation method with overlapped windows and data reuse has been shown to yield on-line HHT biomedical microprocessor. When new data is available, the IMF results are calculated immediately to support real-time biomedical microprocessor. The penalty on accuracy is only less than 3.5%, and 58% multiplication and 73% division computation reductions for the spline coefficients are achieved by the proposed method. In the future, the hardware implementation of on-line HHT processor will be implemented based on the proposed method.

### REFERENCES

- [1] P. B. Colditz and et al., "Digital processing of EEG signals," *IEEE Eng. Med. Bio. Mag.*, vol. 20, no. 5, pp. 21-22, 2001.
- [2] J. P. Zbilut and et al., "Recurrence quantification analysis as a tool for nonlinear exploration of nonstationary cardiac signals," *Med. Eng. Phys.*, pp. 53-60, 2002.
- [3] N. E. Huang and et al., "The empirical mode decomposition and the Hilbert spectrum for nonlinear and non-stationary time series analysis," *in Proc. Royal Society*, pp. 903-995, 1998.
- [4] L. Causa and et al., "Automated sleep-spindle detection in healthy children polysomnograms," *IEEE Trans. Biomed. Eng.*, vol. 57, no. 9, pp. 2135-2146, Sep. 2010.
- [5] L. Wang and et al., "Application of Hilbert-Huang Transform for the study of motor imagery tasks," *IEEE EMBC*, pp. 3848-3851, 2008.
- [6] Y.-L. Wang and et al., "Automatic removal of ocular artifacts from electroencephalogram using Hilbert-Huang Transform," *IEEE Bioinf. and Biomed. Eng.*, pp. 2138-2141, 2008.
- [7] N. ur Rehman and et al., "Application of multivariate empirical mode decomposition for seizure detection in EEG signals," *IEEE EMBC*, pp. 1650-1653, 2010.
- [8] Y.-H. Chen, et al., "Sub-microwatt KNN classifier for implantable closed-loop epileptic neuromodulation system," *Int. Symp. on Bioelectron. and Bioinf.*, pp. 2083-2086, Dec. 2009.
- [9] T.-C. Chen and et al., "1.4μW/channel 16-channel EEG/ECoG processor for smart brain sensor SoC," *Symp. on VLSI Circuits*, pp. 21-22, June 2010.
- [10] A. M. Kamboh and et al., "Area-power efficient VLSI implementation of multichannel DWT for data compression in implantable neuroprosthetics biomedical circuits and systems," *IEEE Trans. on Biomed. Circuits and Systems*, vol. 1, no. 2, pp. 128-135, June 2007.
- [11] Z. Wu and N. E. Huang, "A study of the characteristics of white noise using the empirical mode decomposition method," *Proc. Roy. Soc. London 460A*, pp. 1597-1611, 2004.